NASA Technical Memorandum 101019

A Streamwise Upwind Algorithm for the Euler and Navier-Stokes Equations Applied to Transonic Flows

---

Peter M. Goorjian

September 1988

NASA

National Aeronautics and
Space Administration

A Streamwise Upwind Algorithm for the Euler and Navier-Stokes Equations Applied to Transonic Flows

Peter M. Goorjian, Ames Research Center, Moffett Field, California

September 1988

NASA

National Aeronautics and
Space Administration

Ames Research Center
Moffett Field, California 94035

A Streamwise Upwind Algorithm
for the Euler and Navier-Stokes Equations
Applied to Transonic Flows

Peter M. Goorjian
NASA Ames Research Center
Moffett Field, CA 94035 USA

1. Introduction

A new algorithm has been developed for the Euler and Navier-Stokes equations that uses upwind differencing based on the streamwise direction (Goorjian 1987a, 1987b). This algorithm is time accurate and can be used in codes for calculating unsteady transonic flows over wings. Such codes can be used for the flutter analysis of wings.

In this new algorithm, the coordinate system is locally rotated to align with the streamwise direction. For differencing the convective terms in the streamwise direction, a new form of flux splitting is employed, in which the biasing depends on the local Mach number. In the plane perpendicular to the stream direction, the new flux splitting uses the condition of no flow in that local plane. (The formulas for the differencing in the rotated coordinate system are transformed to the original grid for the calculations.) By using a locally rotated coordinate system, the convective flux vector biasing depends on the total Mach number. Hence, the switching of the flux vector biasing occurs across shock waves and the proper domain of dependence is used in supersonic regions. For comparison, many other upwind methods switch differencing based on Mach number components along coordinate lines. Such criteria allow downstream influences in supersonic regions and switching upstream of shock waves in multidimensional flows. The formulas for the convective flux vector differencing do not contain any user specified parameters. Hence, the amount of numerical dissipation is automatically determined. For viscous flows, calculations of steady flow over a wing using the Navier-Stokes equations were compared with experimental data. Near the body, in a case of separated flow, the calculations showed improvements when compared to calculations that use central differencing with fourth-order dissipation terms.

2. Flux Splitting Algorithm

The thin-layer, Reynolds-averaged, Navier-Stokes equations in generalized curvilinear coordinates are given by

$$\partial_\tau \widehat{Q} + \partial_\xi \widehat{E} + \partial_\eta \widehat{F} + \partial_\zeta \widehat{G} = Re^{-1} \partial_\zeta \widehat{S} \tag{1}$$

where

$$\widehat{Q} = J^{-1} \begin{bmatrix} \rho \\ \rho u \\ \rho v \\ \rho w \\ e \end{bmatrix} , \widehat{E} = J^{-1} \begin{bmatrix} \rho U \\ \rho u U + \xi_x p \\ \rho v U + \xi_y p \\ \rho w U + \xi_z p \\ U(e + p) \end{bmatrix}$$

Here $\widehat{Q}$ is the vector of conservative flow variables and $\widehat{E}$ is the convective flux vector in the ξ direction. See Goorjian (1987a,1987b) for details. In this paper the flux splitting of $\widehat{E}$ will be given. The variables $\widehat{F}$ and $\widehat{G}$ are split in a similar manner. The pressure is given by

$$p = (\gamma - 1) \left[e - (1/2)\rho(u^2 + v^2 + w^2) \right] \qquad (2)$$

and U is the contravariant velocity in the ξ direction.

In solving Eq.(1) at mesh point (i,j,k), the flux vector $\widehat{E}$ at (i+1/2,j,k) is split into $\widehat{E}^+$ and $\widehat{E}^-$, where $\widehat{E}^+$ is evaluated at (i,j,k) and $\widehat{E}^-$ is evaluated at (i+1,j,k). Consider the case where $U \geq 0$; similar formulas hold for $U < 0$. First the split flux will be given for the mass flux component $\widehat{E}_1 = J^{-1}\rho U$.

$$\widehat{E}_1^+ = \frac{1}{2}J^{-1}\rho U \left[1 + (1 - s^+)(\widetilde{U}/q)^2 + s^+(\rho\widetilde{U}/\rho^* q^*)^2 \right]$$
$$- s^+ J^{-1}(1 - 1/\overline{M}^2)(\rho - \rho^*)\widetilde{B}_u(q + q^*)/2 \qquad (3)$$

$$\widehat{E}_1^- = \frac{1}{2}J^{-1}\rho U \left[1 - (1 - s^-)(\widetilde{U}/q)^2 - s^-(\rho\widetilde{U}/\rho^* q^*)^2 \right]$$
$$+ s^- J^{-1}(1 - 1/\overline{M}^2)(\rho - \rho^*)\widetilde{B}_u(q + q^*)/2 \qquad (4)$$

The split energy flux terms $\widehat{E}_5^+$ and $\widehat{E}_5^-$ are obtained by multiplying the respective split mass flux terms $\widehat{E}_1^+$ and $\widehat{E}_1^-$ by the local values of the total enthalpy $(e+p)/\rho$. The split momentum flux components in the x direction are obtained by replacing the mass flux terms $\widehat{E}_1 = J^{-1}\rho U$ in Eqs.(3) and (4) by $\widehat{E}_2 = J^{-1}(\rho u U + \xi_x p)$, which is the x component of the momentum flux from $\widehat{E}$ and also replacing the factor $(q + q^*)/2$ by $((q + q^*)/2)^2(J\widehat{Q}_2/\rho^* q^*)$, where $\widehat{Q}_2 = J^{-1}\rho u$ is the second component of $\widehat{Q}$. Similar substitutions yield the split momentum flux components $\widehat{E}_3^+$, $\widehat{E}_3^-$ and $\widehat{E}_4^+$, $\widehat{E}_4^-$ in the y and z directions, respectively.

The quantities ρ^* and q^* in Eqs.(3) and (4) are local sonic values of the density ρ and speed q. The quantity $\overline{M}$ is an average Mach number between flow quantities and their sonic values. The switches s^+ and s^- switch the flux vector biasing at sonic values, where M = 1. They equal zero for supersonic flow and one for subsonic flow. The quantity $\widetilde{U}$ is the physical component of the velocity corresponding to the contravariant velocity component U, where $(\widetilde{U})^2 = U^2/(|\nabla\xi|)^2$. The variable $\widetilde{B}_u$ is the maximum value of $\rho|U|/\rho^* q^*$ at the two mesh points used to split $\widehat{E}$. For a more detailed explanation of this

splitting, see the papers by Goorjian (1987a,1987b). The only changes in the formulas from Cartesian coordinates for curvilinear coordinates are to use contravariant velocity components such as U and their corresponding physical velocity components such as $\tilde{U}$.

3. Computed Results

Unsteady flow

An unsteady calculation using the Euler equations was made for flow at M = 0.85 over an airfoil whose thickness varies in time. Figure 1 shows the pressure coefficient plots for three times at which the shock wave is increasing in strength and moving downstream as a result of the initial thickening of the airfoil from zero thickness. Notice that the shock profiles at times T = 11.5 and T = 18.25 are sharply captured without any numerical oscillations. The shock profiles at those times contain one and zero mesh points, respectively. Figure 2 shows Mach contour plots at T = 18.25. Notice that the Mach contours are smoothly varying in space. Also notice the tight clustering of the contour lines , where there is a strong transonic shock. This clustering indicates the sharpness of the shock capture.

Wing C: Separated Flow

Figure 3 shows some features of the flow field's tip vortex. It shows traces of particles that were released near the tip. Figure 4 shows a comparison of pressure profiles at the 90% span station, which is the only station for which there is experimental data in the small separated flow region near the tip. At the other four span stations for which there is experimental data, the flow is attached and the two computation methods are in close agreement. Notice in Fig. 4, that the new method, (denoted by TNS-G), produces a shock location and a suction peak that are in closer agreement to the experimental results than the original method, (denoted by TNS). The original method in the TNS code used a coefficient, DIS = 0.2, (a relatively low value), for the fourth-order dissipation. In the region that is influenced by the separated flow, which is from the 90% span station outward to the tip, the two methods showed differences, not only in the shock wave location, but also along the entire upper and lower surfaces.

Figure 5 shows Mach number contours at a height above the wing, where the highest Mach number is reached in the TNS calculation. Notice the higher contour levels reached by the TNS-G method. Also, notice that the TNS results show numerical oscillations in the contour levels at the downstream boundary of this block of the flow domain, whereas the TNS-G results do not. User specification of more dissipation in the TNS calculations to suppress these oscillations; e.g., DIS = 0.64, decreases the region of separated flow. By comparison, the amount of dissipation in the TNS-G results, which is automatically determined, suppresses the oscillations without either diminishing the separated region or diminishing the acceleration of the flow over the leading edge.
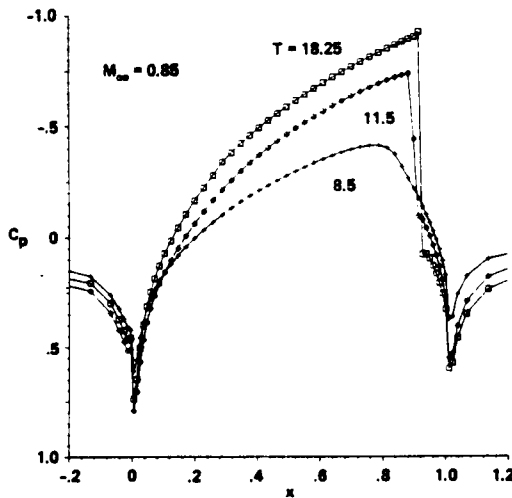
Fig 1. Pressure coefficients for the formation and downstream propagation of the shock wave.
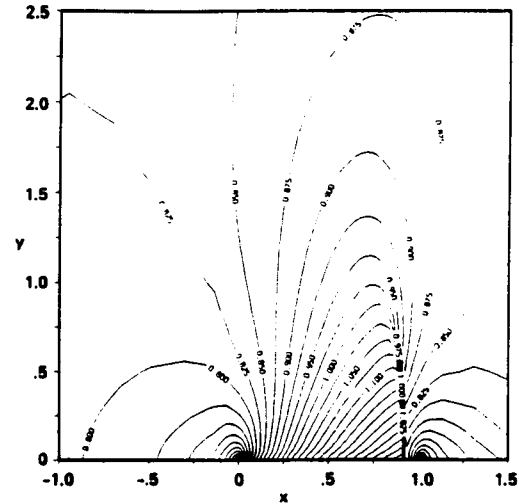
Fig 2. Mach number contours at T = 18.25.
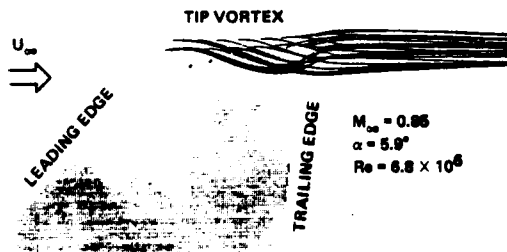
Fig 3. Features of the flow field's tip vortex for Wing C. Plane view of particle traces near the tip.
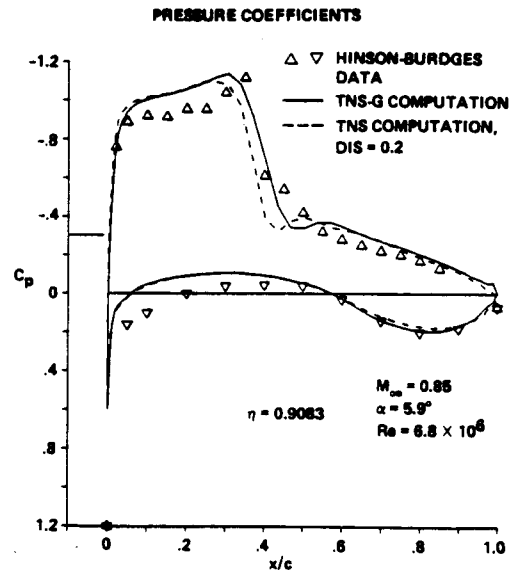
Fig 4. Comparison of experimental and computed pressure coefficients for Wing C.
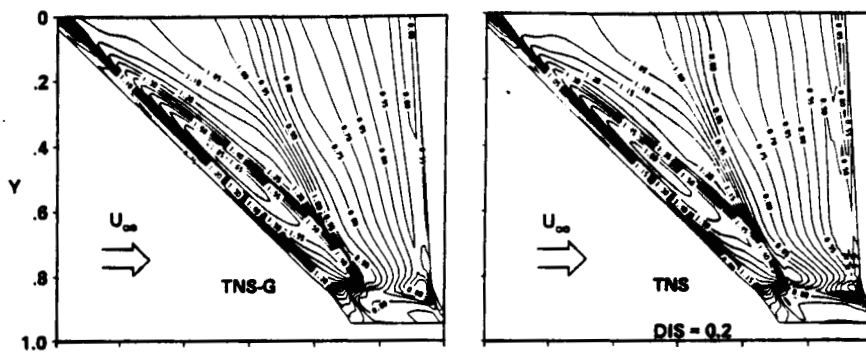
Fig 5. Comparison of Mach contour levels at a height above Wing C.

Figure 6 shows a comparison of boundary layer profiles at the span station, $\eta = 0.9362$, which is near the tip, and at the chord locations $x/c = 0.34$ and $x/c = 0.40$, which are in the shock wave. Notice at both locations that the new method has a fuller velocity profile, which is another indication that near the body, it is automatically adding less numerical viscosity than that used with central differencing.

NACA 0012 Wing: Normal Shock Flow

Next the shock capturing features of the two methods will be compared for flow in which there is a shock wave separating supersonic and subsonic flow; i.e., a normal shock wave. On the wing surface, the pressure profiles obtained by the two methods are similar. However, as the flow field is examined farther away from the wing, the physical viscosity diminishes and the shock capturing features of the two calculations become determined by the differencing of the convective terms.
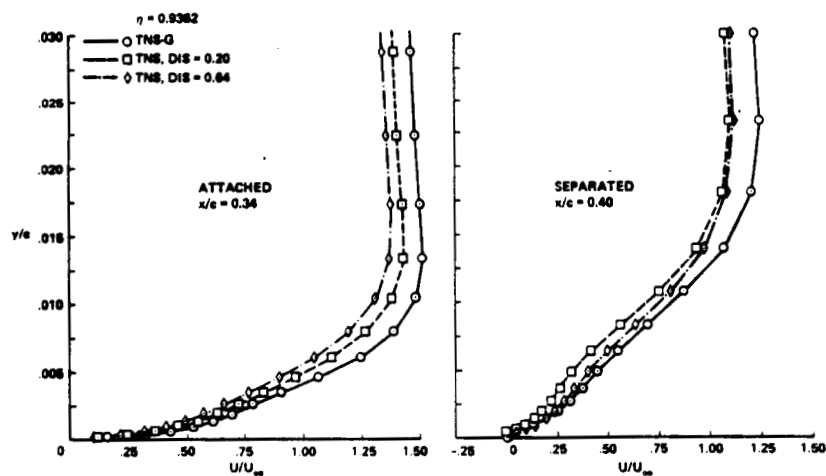
Fig 6. Comparison of the boundary layer profiles for Wing C for the two computational methods.

For comparison, results are presented of pressure coefficients at a height of 0.07 above the wing in units of span length. Figure 7 shows a comparison at two span stations. The TNS method used a value of DIS = 0.64, which is relatively large. Note the improvement obtained in the TNS-G results. The TNS-G results show no overshoots and a sharp capture of the reexpansion singularity. Also the shock is captured at the various span stations with either one or no points in the shock profile. For Euler calculations, these improvements are expected to occur at the wing surface.
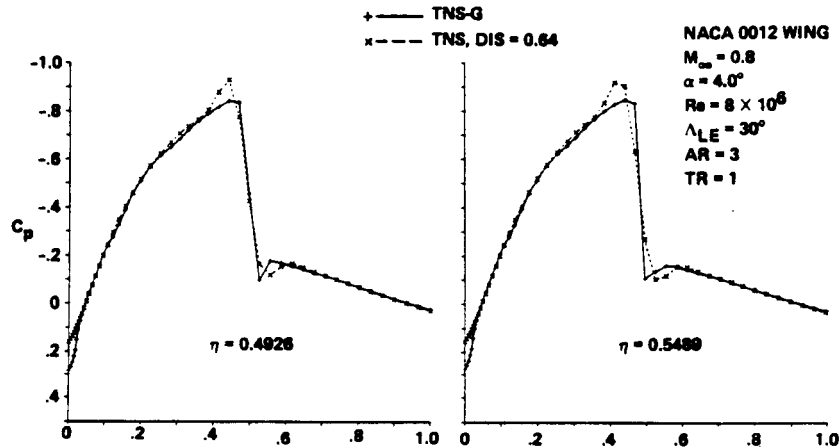
Fig 7. Comparison of the shock capturing properties of TNS-G and TNS. Pressure coefficients in block 2 (inviscid block), at height 0.07 (in span lengths).

References

Goorjian, P. M. (1987a). Algorithm Developments for the Euler Equations with Calculations of Transonic Flows. AIAA Paper 87-0536, AIAA 25th Aerospace Sciences Meeting, Reno, NV, Jan. 12-15, 1987.

Goorjian, P. M. (1987b). A New Algorithm for the Navier-Stokes Equations Applied to Transonic Flows over Wings. AIAA Paper 87-1121-CP, AIAA 8th Computational Fluid Dynamics Conference, Honolulu, Hawaii, June 9-11, 1987.

NASA

Report Documentation Page

1. Report No.	2. Government Accession No.	3. Recipient's Catalog No.
NASA TM-101019		

4. Title and Subtitle	5. Report Date
A Streamwise Upwind Algorithm for the Euler and Navier-Stokes Equations Applied to Transonic Flows	September 1988
	6. Performing Organization Code

7. Author(s)	8. Performing Organization Report No.
Peter M. Goorjian	A-88259
	10. Work Unit No.
	505-60

9. Performing Organization Name and Address	11. Contract or Grant No.
Ames Research Center Moffett Field, CA 94035	
	13. Type of Report and Period Covered

12. Sponsoring Agency Name and Address	Technical Memorandum
National Aeronautics and Space Administration Washington, D.C. 20546-0001	14. Sponsoring Agency Code

15. Supplementary Notes

Point of Contact: Peter M. Goorjian, Ames Research Center, MS 258-1, Moffett Field, CA 94035
(415) 694-6416 or FTS 464-6416

16. Abstract

   A new algorithm has been developed for the Euler and Navier-Stokes equations that uses upwind differencing based on the streamwise direction (Goorjian 1987a, 1987b). This algorithm is time accurate and can be used in codes for calculating unsteady transonic flows over wings. Such codes can be used for the flutter analysis of wings.

   In this new algorithm, the coordinate system is locally rotated to align with the streamwise direction. For differencing the convective terms in the streamwise direction, a new form of flux splitting is employed, in which the biasing depends on the local Mach number. In the plane perpendicular to the stream direction, the new flux splitting uses the condition of no flow in that local plane. (The formulas for the differencing in the rotated coordinate system are transformed to the original grid for the calculations.) By using a locally rotated coordinate system, the convective flux vector biasing depends on the total Mach number. Hence, the switching of the flux vector biasing occurs across shock waves and the proper domain of dependence is used in supersonic regions. For comparison, many other upwind methods switch differencing based on Mach number components along coordinate lines. Such criteria allow downstream influences in supersonic regions and switching upstream of shock waves in multidimensional flows. The formulas for the convective flux vector differencing do not contain any user specified parameters. Hence, the amount of numerical dissipation is automatically determined. For viscous flows, calculations of steady flow over a wing using the Navier-Stokes equations were compared with experimental data. Near the body, in a case of separated flow, the calculations showed improvements when compared to calculations that use central differencing with fourth-order dissipation terms.

17. Key Words (Suggested by Author(s))	18. Distribution Statement
Streamwise upwind algorithm Euler or Navier-Stokes equations Transonic flow applications	Unlimited-Unclassified Subject Category: 02

19. Security Classif. (of this report)	20. Security Classif. (of this page)	21. No. of pages	22. Price
Unclassified	Unclassified	7	A02